J. Electrochem. Sci. Eng. **16** (2026) 3638; https://doi.org/10.5599/jese.3638

Open Access : : ISSN 1847-9286
https://pub.iapchem.org/ojs/index.php/JESE

Original scientific paper

Electrochemical sensing of dopamine using modified glassy carbon electrode

Abbas Sami Abd[1], Aymen Ameen ALwash[2], Hayfaa A Mubarak[3,✉], Ahmed Amer Al-Salman[4] and Huda Hadi Nameh[5]

[1]*Ministry of Education, Qadisiyah Education Directorate, Iraq*
[2]*Department of Prosthetic Dental Techniques, AL-Esraa University, College of Health and Medical Techniques, Baghdad, Iraq*
[3]*Chemical engineering Department, College of Engineering, University of Babylon, Iraq*
[4]*Department of Chemical Engineering, College of Engineering, University of Babylon, Iraq*
[5]*Faculty of Education, Department of Chemistry, University of Hilla, Babylon, 51001, Iraq*

Corresponding Author: ✉*haifaadnan_81@uobabylon.edu.iq*

Received: August 1, 2026; Accepted: September 13, 2026; Published: November 2x, 2026

Abstract

Dopamine (DPM), a crucial neurotransmitter in the central nervous system, regulates motor function, reward circuits, and cognition. Abnormal DPM levels are linked to neurological disorders such as depression, schizophrenia and Parkinson's disease. Electrochemical sensors allow for the fast, sensitive, selective, and economical detection of DPM. In this work, an electrochemical sensor to quantify DPM was designed using a reduced graphene oxide - transition metal oxide, rGO-Cu_2O/Fe_2O_3, nanocomposite. The glassy carbon electrode was then modified, and its electrochemical performance was assessed using cyclic Voltammetry (CV) and differential pulse voltammetry (DPV). On the surface of the modified electrode containing the rGO-Cu_2O/Fe_2O_3 nanocomposite, the oxidation current peak of DPM was twelve times greater than that of the electrode without modification. The findings indicated that the DPM detection limit ranged from 0.005 to 750.0 µM and 2.0 nM. With an effectiveness of 98.2 to 104.0 %, the electrochemical sensor for assessing DPM in DPM injection and urine samples also demonstrates a good recovery. Good selectivity, repeatability, and reproducibility are demonstrated by the produced sensor for DPM measurement.

Keywords

Human central nervous system; neurotransmitter sensing; graphene nanocomposite; transition metal oxides; real samples

Introduction

As a catecholamine neurotransmitter, dopamine (DPM) plays a vital role in the human central nervous system (CNS) [1]. DPM is essential for controlling and coordinating many processes in the cardiovascular, hormonal, renal, and central nervous systems [2]. Additionally, DPM is a brain messenger involved in many physiological processes and is well known for its impact on the regulation and coordination of emotions, pleasure, motivation, movement, and cognition [2]. Some neurological diseases are all associated with low levels of DPM in the brain [3].

Additionally, elevated DPM levels can result in cardiotoxicity, heart failure, elevated blood pressure, and a quicker heartbeat [4]. As a result, tracking and measuring DPM levels can provide important information about patients' health, particularly in the early detection of neurological conditions [4]. The analytical techniques have already been developed for DPM detection [5-14]. They have serious disadvantages, such as susceptibility to interference, complex preparation, high cost, and limited portability. Because of their high sensitivity and affordability, electrochemical sensors are an excellent option in this regard [12-14].

Electrochemical techniques can effectively detect DPM, an electroactive and easily oxidizable compound [14]. Glassy carbon electrodes (GCEs) are frequently used in electroanalytical applications due to their strong chemical resistance, wide potential window, low background current, and mechanical durability [15]. However, because of slow electron-transfer kinetics and poor analyte adsorption, bare GCEs often have low sensitivity, poor selectivity, and surface fouling. Electrocatalytic chemicals or nanomaterials are typically used to modify the GCE to overcome these limitations [16].

Interest in nanostructured materials has increased because of their distinct physicochemical and electrical characteristics [17]. In particular, the development of sensitive and efficient electrochemical sensors that enable rapid identification of target analytes depends on nanostructured materials. When compared to bulk materials, nanocomposites exhibit remarkable characteristics. Nanocomposites are employed in a variety of sectors, including sensors, energy, optics, photonics and more, due to their huge benefits, which include better mechanical, thermal, and chemical properties [18].

Electrochemical sensor research indicates that many nanomaterials, including certain metal oxide nanomaterials, are less expensive, smaller, have a higher surface activity ratio, a larger surface-to-volume ratio, excellent catalytic activity and selective interactions [18]. Transition metal oxides (TMOs) [19] are unique among electrode alternatives because of their high energy density, fast electrochemical kinetics, changeable valence states, and structural stability. Fe_2O_3 magnetic nanoparticles exhibited unique characteristics that significantly deviate from those of bulk phases. Iron oxides have been used for a very long time due to their remarkable ferromagnetic properties [20].

Electronic, magnetic, and optical characteristics of Fe_2O_3 nanoparticles, such as a narrow band gap of 2.2 eV, have broad applications in a variety of industrial processes [20]. With a bandgap of roughly 2.1 eV, cuprous oxide (Cu_2O) is a well-known p-type semiconductor, suitable for applications such as electrocatalysis. For the manufacture of several composite materials, important for electrocatalysis, Cu_2O is a desirable addition.

Its covalent bonding at the basal planes and edges, which increases hydrophilicity, improves dispersion in water [21]. Transition metal oxides are added to two-dimensional layered graphene to create nanocomposites [21]. The electrical connection between transition metal oxides and graphene gives these nanocomposites high catalytic activity and conductivity compared with

(cc) BY

transition metal oxides alone. Transition metal oxides improve catalyst chemical stability by preventing graphene nanosheet agglomeration [22].

Based on these facts, this work investigates the rGO-Cu_2O/Fe_2O_3 nanocomposite for DPM detection. Ultimately, the proposed sensor was used to analyse actual samples, achieving a high level of accuracy.

Experimental

Materials and instrumentation

Every reagent was acquired at the highest available purity and used as supplied, with no further purification. Orthophosphoric acid (0.1 M) was used to prepare the phosphate-buffered solutions (PB), and NaOH was used to adjust the pH to 2.0-9.0. They served as the supporting electrolyte. Differential pulse voltammetry (DPV), cyclic voltammetry (CV) and chronoamperometry were performed on an AUTOLAB PGSTAT 12N potentiostat-galvanostat (Metrohm, The Netherlands). Additionally, the electrochemical cell used in this investigation had three electrode systems: Pt wire as the counter electrode, Ag/AgCl as the reference electrode, and unmodified or modified GCEs as the working electrode (geometric area= 0.0314 cm^2).

Construction of reduced graphene oxide-Cu_2O/Fe_2O_3 nanocomposite

Graphite powder was utilized to produce graphene oxide (GO) using a modified Hummers' process. First, an ultrasonic bath was used to dissolve 50 mg GO in 20 mL ethanol. After adding iron(III) nitrate nonahydrate and copper(II) nitrate trihydrate in a 3:7 ratio, the mixture was agitated until it became a homogenous suspension. The pH was then raised to 11 using a sodium hydroxide (6 M) solution, resulting in a dark, viscous suspension. After being placed in a stainless-steel autoclave and baked at 240 °C for 26 hours, the mixture was centrifuged and extensively cleaned with ethanol and distilled water to achieve a neutral pH. Finally, the final product was dried for 16 hours at 50 °C.

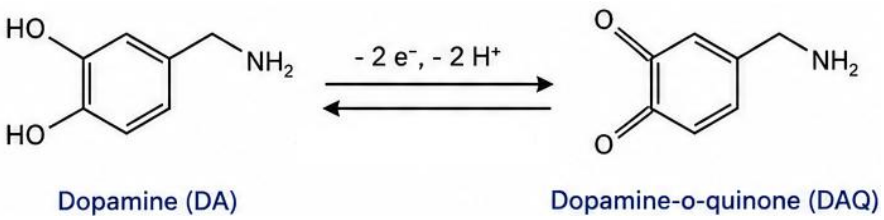
Fabrication of modified electrode

A GCE was polished to achieve a mirror-like surface before alteration. After removing adsorbed particles by successive ultrasonication in ethanol and distilled water, the polished electrode was dried. 2 mg of the produced nanocomposite was dispersed in 500 µL of water under ultrasonication to create a suspension of rGO-Cu_2O/Fe_2O_3 (GCF) nanocomposite for electrode modification. Using a micropipette, 5 µL of this homogeneous suspension was drop-cast onto the cleaned GCE. The modified electrode was left to dry. Afterward, electrochemical research and sensing applications were conducted using the resulting GCF/GCE.

Results and discussion

Evaluation of the pH effect

Because it affects both electrochemical reactions at the electrode interface and the sensor's overall performance, electrolyte pH is a crucial component of electrochemical sensors. Changes in electrolyte pH can dramatically alter the kinetics and thermodynamics of electrochemical processes. DPM oxidation on the GCF/GCE surface is influenced by the pH (Scheme 1). To investigate this, DPVs for the modified electrode in a 100.0 µM DPM solution with phosphate buffer at pH levels ranging from 4.0 to 9.0 were acquired.



Scheme 1. *Electrooxidation mechanism for DMP on GCF/GCE*

The oxidation current for DPM increases with pH, peaks at pH 7.0, and then falls at higher pH values. Therefore, the ideal pH for studies was determined to be 7.0. Furthermore, we noted that as pH increases, peak potential shifts toward lower potentials. This shift shows that the peak potential depends linearly on pH.

Electrochemical behaviour of dopamine on the reduced graphene oxide-Cu_2O/Fe_2O_3 nanocomposite/glassy carbon electrode

The potential application of GCF/GCE for electrooxidation and CV-based DPM measurements was investigated. The response for the oxidation of DPM on (a) bare GCE and (b) GCF/GCE in PB is shown in Figure 1.

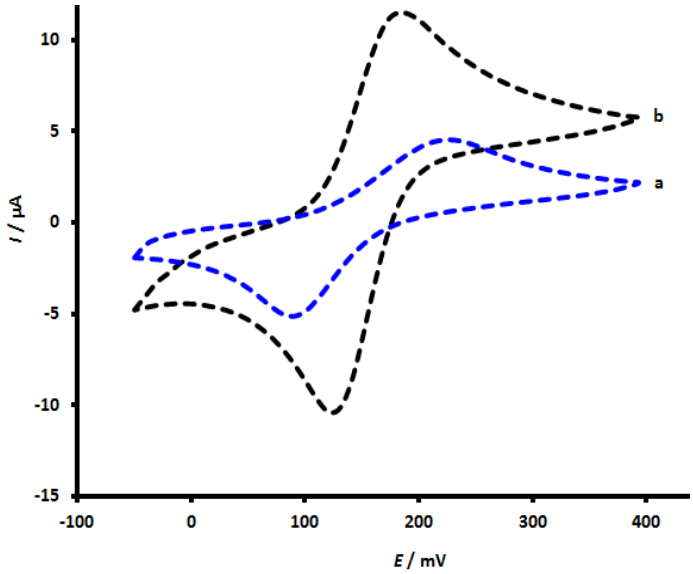


Figure 1. *CVs (50 mV s^{-1}) of unmodified a - GCE and b - GCF/GCE in PB containing 200.0 µM DMP*

The anodic and cathodic currents increase from 4.5 to 11.5 µA and from -5.1 to -10.4 µA, respectively, as illustrated in Figure 1. Peak-to-peak potential separation ($\Delta E_p = E_{pa} - E_{pc}$) also drops from 0.14 to 0.06 V.

Influence of scan rate

Using CV, the effect of different scan rates on DPM electrochemistry was assessed. Figure 2 displays the equivalent CV responses of GCF/GCE. According to the measured CVs, the DPM redox peak currents improved as the scan rate increased. In addition, it is evident from Figure 3 that the anodic peak current (I_{pa}) and cathodic peak current (I_{pc}) of DPM revealed a linear dependence on the square root of the scan rate, $\upsilon^{1/2}$. This showed that the redox process of DPM at the GCF/GCE is diffusion-controlled.

(cc) BY

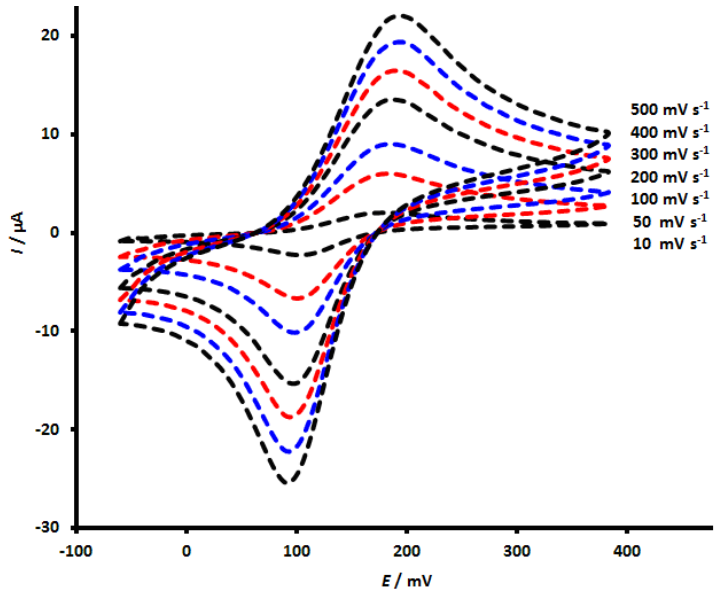


Figure 2. *CVs of GCF/GCE in PB containing 100.0 µM DMP at different scan rates*

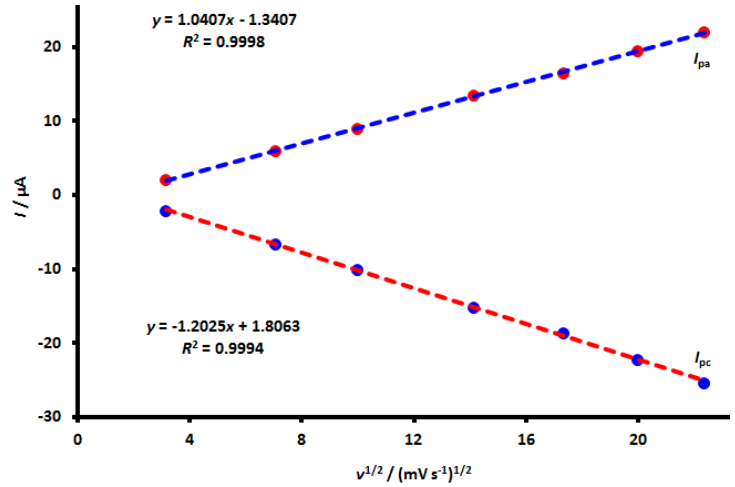


Figure 3. *Variation* I_{pa} *and* I_{pc} vs. $v^{1/2}$ *for CVs in Figure 2*

Chronoamperometric studies

Chronoamperometry was used to estimate the diffusion coefficient (*D*) of DPM at the GCF/GCE since its electrochemical reaction is diffusion-controlled (potential step = 220 mV). Chrono-amperograms for various DPM concentrations at the GCF/GCE are shown in Figure 4.

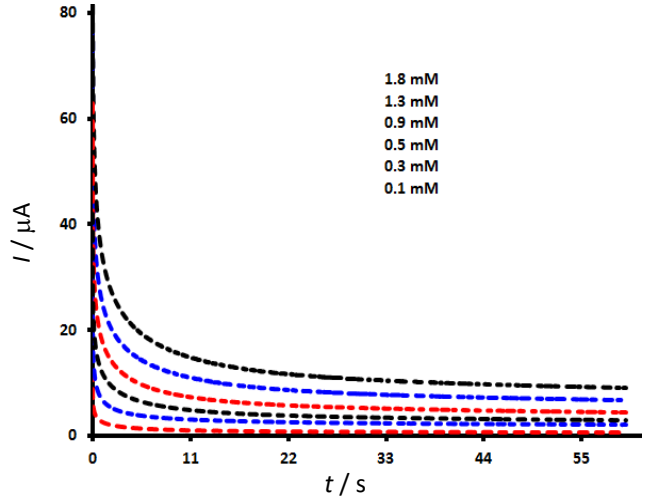


Figure 4. *Chronoamperograms obtained at GCF/GCE in PB for different concentrations of DPM*

http://doi.org/10.5599/jese.3638

The Cottrell Equation (1) was used to calculate *D*:

$$I = nFACD^{1/2}\pi^{-1/2}t^{-1/2} \quad (1)$$

The bulk concentration is represented by *C* in this equation, while the surface area and number of electrons are represented by *A and n*. The linearity between I and $t^{-1/2}$ was validated by the experimental *I vs.* $t^{-1/2}$ plots (Figure 5A). The slopes were then plotted against the respective DPM concentrations (Figure 5B), from which *D* was found to be 5.4×10^{-6} cm^2 s^{-1}.

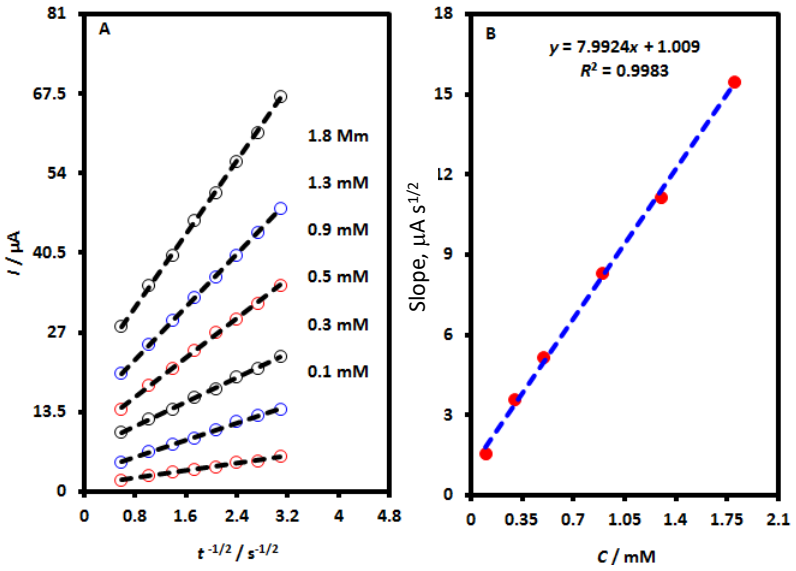


Figure 5. *(A) Plots of* I vs. $t^{-1/2}$*, (B) plots of slope* vs. C_{DPM}

Quantitative measurements of dopamine at reduced graphene oxide-Cu_2O/Fe_2O_3 nanocomposite/glassy carbon electrode sensor using differential pulse voltammetry method

Figure 6 shows the DPVs for DPM oxidation in PB measured at the GCF/GCE.

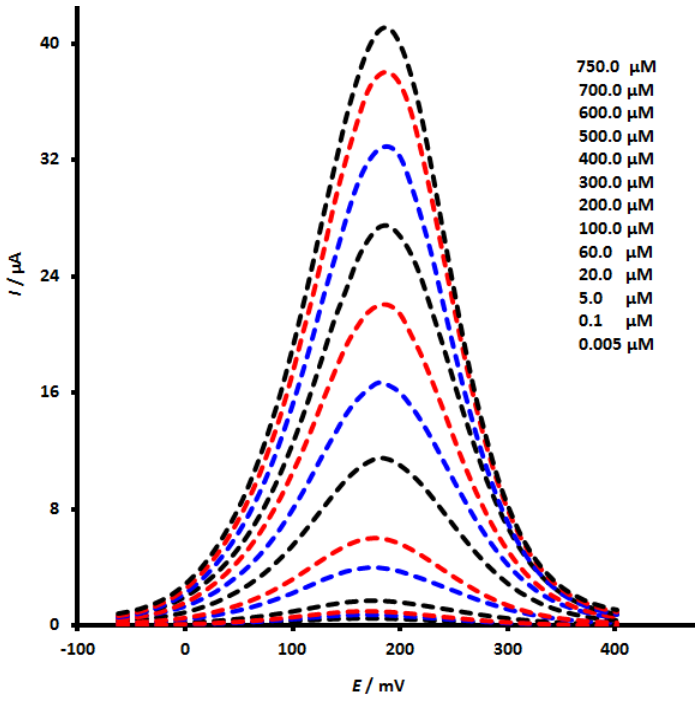


Figure 6. *DPVs of GCF/GCE in PB containing different concentrations of DPM.*

The peak currents for DPM increased gradually with its concentration using the determined optimal parameters (Figure 7). Over a range of 0.005 to 750.0 µM, linear dependence between the peak current and the DPM concentration was found.

CC BY

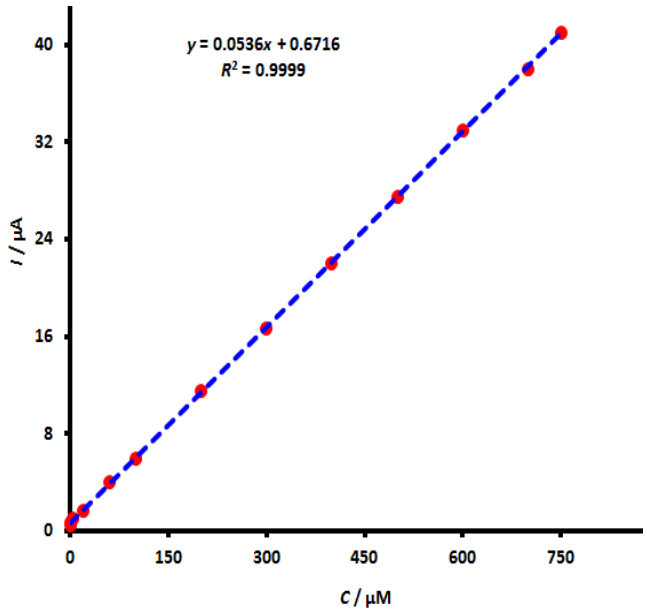


Figure 7. *Plot of the peak current as a function of DPM concentration*

Equation (2) was used to calculate the limit of detection (LOD):

$$LOD = 3S_{Blank}/m \quad (2)$$

where S_{Blank} is the standard deviation of the blank solution (n = 10) and m is the slope of the calibration curve. LOD was determined to be 0.002 Mm.

Repeatability, reproducibility and stability study

Five GCF/GCE units were tested using a 50.0 µM DPM solution under identical conditions (pH 7.0) to assess the sensor's reproducibility. The relative standard deviation (RSD) was 2.1 %. The great reproducibility of the GCF/GCE in DPM analysis is demonstrated by this RSD value. Additionally, the response currents of 100.0 µM DPM were compared by preparing the other five GCF/GCEs under identical conditions. The modified electrode's remarkable repeatability was demonstrated by an RSD as low as 3.6 %. The GCF/GCE electrode was kept in ambient conditions for the long-term stability evaluation using DPV. The peak current for 100.0 µM DPM at the modified electrode remained 94.2 % of its initial response after 7 days, 92.9b % after 14 days, and 91.0 % after 21 days. These results validate the suggested sensor's exceptional long-term stability.

Interference study

One of the most important features of a novel sensor is selectivity. Under ideal circumstances, precisely at 50.0 µM DPM at pH 7.0, the impact of different substances that might interfere with the measurement of DPM was examined. The greatest concentration of an interfering substance that resulted in a DPM measurement error of less than ±5 % was identified as the tolerance limit.

The findings indicate that citric acid, sucrose, ethanol, glucose, methanol, acetaminophen, uric acid, tryptophan, methionine, SO_4^{2-}, Mg^{2+}, Cl^-, NH_4^+, K^+, CO_3^{2-}, and Na^+ did not affect the measurement of DPM when present at equivalent concentrations alongside DPM. On the other hand, ascorbic acid interfered with DPM quantification when present in similar amounts. Nevertheless, the enzyme ascorbate oxidase, which preferentially catalyses the oxidation of ascorbic acid, could reduce the interference caused by ascorbic acid.

Analysis of urine sample and dopamine injection

This study evaluated how well the developed sensor functioned when analysing actual samples. Determination of DPM in the urine and DPM injection samples was examined for this purpose. First,

the amount of DPM in the prepared samples was quantified, and the DPV responses of the GCF/GCE were noted from unspiked samples. Next, known quantities of DPM were spiked into the samples, and the corresponding DPV current responses were recorded. The recoveries were calculated using the conventional addition process. Table 1 shows that the constructed sensing platform's high accuracy was demonstrated by the satisfactory recovery values, which ranged from 98.2 to 104.0 %.

Table 1. *GCF/GCE estimation of DPM in real samples (*n*=5)*

Sample	Amount, μM		Recovery, %	RSD, %
	Spiked	Found		
DPM injection	0	3.4	-	3.6
	2.0	5.5	101.8	2.7
	4.0	7.3	98.6	1.9
	6.0	9.6	102.1	2.4
	8.0	11.4	99.1	2.9
Urine	5.5	5.4	98.2	2.5
	7.5	7.8	104.0	3.7
	9.5	9.4	98.9	2.6
	11.5	11.6	100.9	1.8

Conclusion

In conclusion, our work demonstrated of an electrochemical sensing platform based on rGO-Cu_2O/Fe_2O_3/GCE (GCF/GCE) that may be used to identify DPM traces in actual materials. When compared to other electrodes, the CV findings demonstrated a significant improvement in oxidation signal enhancement and overpotential reduction at the surface of GCF/GCE. With a linear range of 0.005 to 750.0 μM, a low LOD of 0.002 μM, the developed sensor can detect DPM concentration by DPV. Additionally, the GCF/GCE sensor was used to measure DPM concentration in DPM injection and urine samples. According to the analysis, the recovery values had RSD values ≤ 3.6 % and ranged from 98.2 to 104.0 %.

References

[1] M. Li, L. Zhou, X. Sun, Y. Yang, C. Zhang, T. Wang, F. Fu, Dopamine, a co-regulatory component, bridges the central nervous system and the immune system, *Biomedicine & Pharmacotherapy* **145** (2022) 112458. https://doi.org/10.1016/j.biopha.2021.112458

[2] M. Cohen, S. Atzil, A metabolic framework for reward: Redefining dopamine and opioids as physiological agents, *Neuroscience & Biobehavioral Reviews* **184** (2026) 106608. 10.1016/j.neubiorev.2026.106608

[3] J. N. Joyce, A. M. Murray, H. I. Hurtig, G. L. Gottlieb, J. Q. Trojanowski, Loss of dopamine D2 receptors in Alzheimer's disease with parkinsonism but not Parkinson's or Alzheimer's disease, *Neuropsychopharmacology* **19(6)** (1998) 472-480. https://doi.org/10.1016/S0893-133X(98)00044-X

[4] R. Hadar, M. Voget, V. Vengeliene, J. K. Haumesser, C. van Riesen, Y. Avchalumov, R. Spanagel, C. Winter, Altered neural oscillations and elevated dopamine levels in the reward pathway during alcohol relapse, *Behavioural Brain Research* **316** (2017) 131-135. https://doi.org/10.1016/j.bbr.2016.08.045

[5] M. A. Ramadan, I. Almasri, G. Khayal, Spectrophotometric determination of dopamine in bulk and dosage forms using 2, 4-dinitrophenylhydrazine, *Turkish Journal of Pharmaceutical Sciences* **17(6)** (2020) 679. https://doi.org/10.4274/tjps.galenos.2019.25902

[6] S. S. Tessema, H. Liu, A. Abdussalam, T. Lijalem, A. A. Alboull, A. Hussain, S. Hanif, G. Xu, Co_3O_4/CuO hollow nanocages as effective bimetallic nanocatalysts of luminol/H_2O_2

(cc) BY

chemiluminescence for dopamine detection, *Microchemical Journal* **224** (2026) 117924. https://doi.org/10.1016/j.microc.2026.117924

[7] A. Naccarato, E. Gionfriddo, G. Sindona, A. Tagarelli, Development of a simple and rapid solid phase microextraction-gas chromatography-triple quadrupole mass spectrometry method for the analysis of dopamine, serotonin and norepinephrine in human urine, *Analytica Chimica Acta* **810** (2014) 17-24. https://doi.org/10.1016/j.aca.2013.11.058

[8] X. Wang, L. Wang, M. Wu, Y. Zheng, R. Wang, T. Shao, S. Zeng, A. Li, R. Li, Q. Yue, Portable and intelligent ratio fluorometry and colorimetry for dual-mode detection of dopamine based on B, N-codoped carbon dots and machine learning, *Talanta* **294** (2025) 128288. https://doi.org/10.1016/j.talanta.2025.128288

[9] M. Tsunoda, C. Aoyama, H. Nomura, T. Toyoda, N. Matsuki, T. Funatsu, Simultaneous determination of dopamine and 3, 4-dihydroxyphenylacetic acid in mouse striatum using mixed-mode reversed-phase and cation-exchange high-performance liquid chromatography, *Journal of Pharmaceutical and Biomedical Analysis* **51** (2010) 712-715. https://doi.org/10.1016/j.jpba.2009.09.045

[10] X. Wang, Y. Chen, P. Jia, Q. An, Li X., Sun J., Z. Su, Rapid ratiometric fluorescence detection of dopamine hydrochloride in pork extracts using a Zn/Cd bimetallic MOF, *Microchemical Journal* **229** (2026) 119336. https://doi.org/10.1016/j.microc.2026.119336

[11] Y. Zhao, S. Zhao, J. Huang, F. Ye, Quantum dot-enhanced chemiluminescence detection for simultaneous determination of dopamine and epinephrine by capillary electrophoresis, *Talanta* **85(5)** (2011) 2650-2654. https://doi.org/10.1016/j.talanta.2011.08.032

[12] A. O. Imarah, N. Hasan, M. G. Alabbasi, ZnO-modified carbon paste electrode for electrochemical sensing of dopamine in the presence of tyrosine, *ADMET and DMPK* **13** (2025) 3010. https://doi.org/10.5599/admet.3010

[13] Chen H. C., Huang WW, Lin Y. S., Chang H. H. Gold-core silver-shell nanoparticles modified magnetic-based metal-organic frameworks for dopamine sensing electrodes: Magnetic Fe-based and LSPR gain mechanisms, *Journal of Alloys and Compounds* **1065** (2026) 188120. https://doi.org/10.1016/j.jallcom.2026.188120

[14] A. H. Gatea, A. S. Ajel, R. M. Mhaibes, A new method for measuring dopamine in the presence of uric acid employing a carbon paste electrode modified with the UiO-66 metal organic framework-graphene oxide nanocomposite, *ADMET and DMPK* **13** (2025) 2593. https://doi.org/10.5599/admet.2593

[15] W. T. Wahyuni, S. A. Hasnawati Ta'alia, A. Y. Akbar, B. R. Elvira, I. Rahmawati, R. A. Wahyuono, B. R. Putra, Electrochemical sensors based on the composite of reduced graphene oxide and a multiwalled carbon nanotube-modified glassy carbon electrode for simultaneous detection of hydroquinone, dopamine, and uric acid, *RSC Advances* **14(38)** (2024) 27999-28016. https://doi.org/10.1039/d4ra05537c

[16] J. Chen, X. Ran, X. Ding, D. Zhang, Dual electrochemical quantitative analysis of dopamine based on flow injection amperometry with double glassy carbon electrodes, *Electrochemistry Communications* **151** (2023) 107511. https://doi.org/10.1016/j.elecom.2023.107511

[17] L. Meng, C. Qing, Y. Wang, Y. Cai, H. Wei, M. Zhang, A UiO-66-derived nano-separation microelectrode for in vivo dopamine sensing with high sensitivity and selectivity, *Chemical Communications* **62(44)** (2026) 11184-11187. https://doi.org/10.1039/d6cc01892k

[18] L. M. Ntuli, A. Nyembwe, G. Mwengula, T. Munonde, J. Mulopo, Recent advances in metal oxide, bimetallic nanocomposites, metal-organic frameworks (MOFs), and non-invasive technologies for biofluid-based glucose sensors: A comprehensive review, *International Journal of Electrochemical Science* **20** (2025) 101184. https://doi.org/10.1016/j.ijoes.2025.101184

[19] A. S. Adekunle, E. O. Aluko, E. S. Eluwale, M. O. Bello, M. J. Madito, F. G Xolile., T. T. Nkambule, P. R. Makgwane, B. B. Mamba, Transition Metal Oxides as Electrode Materials for

Advanced Energy Storage-A Decade of Research on Batteries and Supercapacitors, *Chemical Physics Impact* **13** (2026) 101112. https://doi.org/10.1016/j.chphi.2026.101112

[20] J. Zoubir, N. Bougdour, C. Radaa, A. Idlahcen, I. Bakas, A. Assabbane, Elaboration of a novel nanosensor using nanoparticles of α-Fe_2O_3 magnetic cores for the detection of metronidazole drug. Urine human and tap water, *Sensors International* **229** (2022) 100160. https://doi.org/10.1016/j.sintl.2022.100160

[21] F. M. Altalbawy, Q. A. Mohammed, H. K. Jaafar, N. Fayzullaev, M. A. Vora, S. Ganesan, R. Sharma, G. Durga, P. Sharma, S. Amiri, pH-dependent rGO/Cu-Cu_2O electrodes with a porous PVA/PEO film for high-sensitivity non-enzymatic glucose sensing: a COMSOL multiphysics study, *RSC Advances* **16(19)** (2026) 17536-17554. https://doi.org/10.1039/d5ra09249c

[22] S. S. Gaikwad, S. S. Warule, M. D. Babar, S. K. Pardeshi, S. S. Dahiwale, M. A. More, Facile synthesis of Cu_2O-rGO nanocomposite with enhanced electrochemical performance as a supercapacitor electrode, *Next Materials* **10** (2026) 101430. https://doi.org/10.1016/j.nxmate.2025.101430

©2026 by the authors; licensee IAPC, Zagreb, Croatia. This article is an open-access article distributed under the terms and conditions of the Creative Commons Attribution license (http://creativecommons.org/licenses/by/4.0/)